Rankine-Hugoniot Relations in Relativistic Combustion Waves

Yang Gao¹ and Chung K. Law¹,²

¹ Center for Combustion Energy and Department of Thermal Engineering, Tsinghua University, Beijing, 100084, China

> ² Department of Mechanical and Aerospace Engineering, Princeton University, Princeton, NJ 08544-5263, USA

> > cklaw@Princeton.EDU

Received;	accepted
7	

ABSTRACT

As a foundational element describing relativistic reacting waves of relevance to astrophysical phenomena, the Rankine-Hugoniot relations classifying the various propagation modes of detonation and deflagration are analyzed in the relativistic regime, with the results properly degenerating to the non-relativistic and highly-relativistic limits. The existence of negative-pressure downstream flows is noted for relativistic shocks, which could be of interest in the understanding of the nature of dark energy. Entropy analysis for relativistic shock waves are also performed for relativistic fluids with different equations of state (EoS), denoting the existence of rarefaction shocks in fluids with adiabatic index $\Gamma < 1$ in their EoS. The analysis further shows that weak detonations and strong deflagrations, which are rare phenomena in terrestrial environments, are expected to exist more commonly in astrophysical systems because of the various endothermic reactions present therein. Additional topics of relevance to astrophysical phenomena are also discussed.

Subject headings: hydrodynamics: shock waves — ISM: kinematics and dynamics

1. Introduction

The classical theory of combustion waves is well established in the study of reactive fluid dynamics (Williams 1985; Zel'dovich et al. 1985; Law 2006). Different from hydrodynamic shock waves which have been extensively studied, supersonic detonations and subsonic deflagrations are sustained by reactions in the fronts of fluid discontinuities (see, e.g., Landau & Lifshitz 1959; Williams 1985), and as such are expected to yield rich varieties of fluid dynamical responses.

Axford and Newman (Axford 1961; Newman & Axford 1968) first adopted the concept of reactive fluid dynamics in astrophysics by considering the dynamics of the hydrogen ionization fronts around stars. Blandford & Ostriker (1978, 1980) advanced the mechanism of particle acceleration through astrophysical shocks such as those in supernova systems, which in principle should also bear the dynamics of reactive flows. Indeed, it is now commonly believed that nuclear deflagration and detonation waves support the explosion of Type Ia supernovae (Arnett 1969; Hillebrandt & Niemeyer 2000; Gamezo et al. 2003, 2005), recognizing nevertheless that the transition mechanism from deflagration to detonation is still not clear. Additional studies of astrophysical processes that have suggested/invoked combustion processes include relativistic detonation waves as a possible mechanism for the false vacuum decay (Steinhardt 1982), relevant for the microwave background fluctuations (Gibson 2005) in the early universe; the fireball model for the γ -ray burst (Mészáros 2002) involving relativistic γ photons and electron/positron pairs; and the unique role of the ISM shocks in various chemical processes in molecular clouds, particularly in early-phase star formations (e.g., McKee & Ostriker 2007; Flower & des Forêts 2010) as observed in detail by Herschel and other facilities. Furthermore, a recent study (Gao & Law 2011) on the evolution of supernovae remnants has also incorporated reaction to account for the accelerative expansion of the Crab Nebula.

It is thus clear that integration of combustion theory offers rich potential in the study of astrophysical phenomena.

To adopt reactive fluid dynamics in the study of astrophysical systems, a general form of combustion wave theory in relativistic fluids is needed. While theories of relativistic shock waves (Taub 1948) and detonation waves in highly-relativistic fluids (Steinhardt 1982) have been advanced, and the relativistic shock waves for radiating fluids (Cissoko 1997) and for fluids in magnetic fields (Mallick 2011) have been presented, a general analysis of combustion waves describing subsonic deflagration as well as supersonic detonation waves, for all relativistic fluids, has not been performed. Consequently, as a first, necessary step, we shall integrate the essential features of relativistic fluids (Landau & Lifshitz 1959; Anile 1989) and combustion waves (Williams 1985; Law 2006), within the context of the Rankine-Hugoniot relations, and identify the various possible relativistic combustion waves and their properties. The relativistic theory of deflagration and detonation waves has also been studied in quark-gluon plasmas using the bag equation of state for the quark matter (Gyulassy et al. 1984), which is a useful reference for the present study of combustion waves in a Synge gas (Synge 1957) with the adiabatic index Γ for more general astrophysical applications.

Since the relativistic shock is an important component in relativistic flows, it will be separately studied first in Section 2, in which an interesting solution involving negative pressure in the downstream fluid is identified, and entropy analysis to the shocks are founded. In Section 3, the general relativistic form of deflagration and detonation waves is presented, with its proper degeneracy to the non-relativistic and highly-relativistic limits. Detonation and deflagration waves, as well as special cases of Chapman-Jouguet waves and

¹Here highly-relativistic fluids refer to those hydrodynamic systems whose speed of fluid particles are very close, or equal, to the speed of light.

isobaric waves are analyzed therein. The possible existence of weak detonations and strong deflagrations in relativistic astrophysical environments is then discussed, which is followed by summary of the present work, in Section 4.

2. Relativistic shock waves

We first briefly outline the fundamentals of relativistic fluid dynamics and the theory of relativistic shock waves (Taub 1948; Landau & Lifshitz 1959; Liang 1977).

2.1. Basic equations governing the relativistic gas

Based on the energy-momentum tensor in the local rest frame of a relativistic fluid

$$T^{ik} = \begin{pmatrix} e & 0 & 0 & 0 \\ 0 & p & 0 & 0 \\ 0 & 0 & p & 0 \\ 0 & 0 & 0 & p \end{pmatrix}, \tag{1}$$

momentum and energy conservations across a shock front are:

$$\omega_1 u_1^2 + p_1 = \omega_2 u_2^2 + p_2 \tag{2}$$

and

$$\omega_1 \gamma_1 u_1 = \omega_2 \gamma_2 u_2, \tag{3}$$

respectively (Landau & Lifshitz 1959; Steinhardt 1982). Here e is the fluid energy density, which includes the rest-frame energy nm_0c^2 of the fluid particles and the specific internal energy ϵ (see Equation (6)), p is the pressure of the fluid, $\omega = e + p$ the specific enthalpy per unit volume, m_0 the rest mass of one particle and n the particle number density which can be the number density of any charge (e.g., baryon number or lepton number)

that is conserved across the shock front. The four-velocity u of the fluid has the form $u = \beta \gamma$, where $\beta = v/c$ is the velocity in unit of the speed of light and $\gamma = 1/(1-\beta^2)^{1/2}$ is the Lorentz factor. Subscripts 1 and 2 denote upstream and downstream quantities, respectively. The particle number conservation

$$n_1 u_1 = n_2 u_2 (4)$$

is a complementary condition of continuity across the shock.

For analysis pertinent to the stellar interior, the ISM or intergalactic media (IGM), and the early universe, the relativistic ideal gas is described by the following equation of state (EoS) with the adiabatic index Γ (i.e., the Synge gas, cf. Synge 1957; Lanza et al. 1982; Cissoko 1997):

$$\Gamma = 1 + \frac{p}{\rho \epsilon},\tag{5}$$

where $\rho = nm_0$ is the rest-frame mass density and ϵ the specific internal energy (cf. Equation(6)). Then the fluid energy density can be written as

$$e = \rho(c^2 + \epsilon) = nm_0c^2 + \frac{1}{\Gamma - 1}p,$$
(6)

which can also be considered as the definition of the specific internal energy ϵ . Using the EoS (5), the specific enthalpy has the following form (Kennel & Coroniti 1984),

$$\omega = e + p = nm_0c^2 + \frac{\Gamma}{\Gamma - 1}p. \tag{7}$$

The EoS with $4/3 \le \Gamma \le 5/3$ (Taub 1948; Anile 1989) is a general form for relativistic fluids. In the highly-relativistic regime ($\Gamma = 4/3$), the internal energy greatly exceeds the rest-frame energy of the particle, i.e., $\epsilon \gg c^2$, and the fluid is radiation dominant with $p = \frac{1}{3}\rho\epsilon = \frac{1}{3}e$. This is the EoS used in Steinhardt (1982) in the study of the bubble growth during the false vacuum decay in the early evolution phase of the universe. In the non-relativistic extreme ($\Gamma = 5/3$, cf. Anile 1989), $\epsilon \ll c^2$, the EoS assumes the form

 $p = \frac{2}{3}\rho\epsilon$. Comparing this expression with the classical ideal gas law $p = \rho kT$, with k being the Boltzmann constant, the internal energy is just the kinetic energy $\epsilon = \frac{3}{2}kT$ for a monatomic gas in non-relativistic fluids. Another special EoS with $\Gamma = 2/3$ accounting for the dark energy in the universe will be discussed in Section 2.3.

The sound speed in relativistic fluids is given by (cf. Landau & Lifshitz 1959)

$$v_{\rm s} = c\sqrt{\frac{\partial p}{\partial e}},\tag{8}$$

whose four-velocity is $u_s = \beta_s \gamma_s = \frac{v_s}{c} (1 - (\frac{v_s}{c})^2)^{-1/2}$. Following the above discussion, we have $v_s = c/\sqrt{3}$ in the highly-relativistic regime and $v_s = \sqrt{\frac{\partial p}{\partial \rho}}$ in the non-relativistic regime.

2.2. The relativistic shock adiabat

By defining a variable $x = \omega/n^2$ for fluids in both sides of the wave front, we readily obtain the expressions for the particle flux $(j = n_1 u_1 = n_2 u_2)$ by considering momentum conservation (2) and particle flux conservation (4)

$$-j^2 = \frac{p_2 - p_1}{x_2 - x_1},\tag{9}$$

and the so-called shock adiabat by additionally considering the energy conservation (3) (cf. Taub 1948; Landau & Lifshitz 1959; Steinhardt 1982):

$$x_2\omega_2 - x_1\omega_1 = (p_2 - p_1)(x_2 + x_1). (10)$$

Referring to the form of the specific enthalpy (7) under the EoS, the variable x can be expressed as

$$x = \frac{1}{n^2} \left(n m_0 c^2 + \frac{\Gamma}{\Gamma - 1} p \right) = \frac{m_0^2 c^2}{\rho} + \frac{\Gamma}{\Gamma - 1} \frac{m_0^2 p}{\rho^2}.$$
 (11)

Introducing Equation (11) to the particle flux (9), we obtain the Rayleigh relation for relativistic fluids, accounting for the conservation of number density and momentum:

$$(\hat{p}-1) = -u_1^2 \left[\hat{c}^2(\hat{V}-1) + \frac{\Gamma}{\Gamma-1} (\hat{p}\hat{V}^2 - 1) \right]. \tag{12}$$

Here $V=1/\rho$ is the specific volume, and notations with hats are reduced variables, i.e., $\hat{p}=p_2/p_1$, $\hat{V}=V_2/V_1$ and $\hat{c}=c/\sqrt{p_1V_1}$. In the limit of $\hat{c}\to\infty$ and $u_1\to 0$, the Rayleigh relation degenerates to that in the non-relativistic regime (cf. Landau & Lifshitz 1959):

$$M_1^2 = -\frac{\hat{p} - 1}{\Gamma(\hat{V} - 1)},\tag{13}$$

where $M = v/\sqrt{\Gamma p/\rho}$ is the non-relativistic Mach number; while in the limit of $\hat{c} \to 0$, it assumes the highly-relativistic form:

$$u_1^2 = -\frac{(\Gamma - 1)(\hat{p} - 1)}{\Gamma(\hat{p}\hat{V}^2 - 1)}.$$
 (14)

By introducing x given by (11) to the shock adiabat (10), we derive the Hugoniot relation for relativistic shocks:

$$\hat{c}^2 \left[\frac{\Gamma + 1}{\Gamma - 1} (\hat{p}\hat{V} - 1) - (\hat{p} - \hat{V}) \right] = \frac{\Gamma}{\Gamma - 1} \hat{p} (1 - \hat{V}^2) - \frac{\Gamma}{(\Gamma - 1)^2} (\hat{p}^2 \hat{V}^2 - 1). \tag{15}$$

The Hugoniot relation additionally takes into account of energy conservation (3) and as such describes all possible discontinuities across a shock by considering all conservation equations. In the non-relativistic extreme of $\hat{c} \to \infty$ and $u_1 \to 0$, Equation (15) reduces to (Landau & Lifshitz 1959)

$$\left(\hat{p} + \frac{\Gamma - 1}{\Gamma + 1}\right)\left(\hat{V} - \frac{\Gamma - 1}{\Gamma + 1}\right) = \frac{4\Gamma}{(\Gamma + 1)^2}.$$
 (16)

In the highly-relativistic extreme of $\hat{c} \to 0$, the RHS of Equation (15) vanishes, yielding

$$\hat{p}\hat{V}^2 = \frac{(\Gamma - 1)\hat{p} + 1}{(\Gamma - 1) + \hat{p}}.$$
(17)

The highly-relativistic shock adiabat, i.e., Rayleigh and Hugoniot relations, have been derived and discussed in, e.g., Steinhardt (1982).

Hugoniot lines represented by Equation (15) are illustrated in Figure 1 for non-relativistic, relativistic and highly-relativistic fluids. Along reference line a, it is seen that

the density increase is higher for relativistic fluids than for non-relativistic fluids for the same pressure enhancement ratio across the compression shock. And along reference line b the pressure reduction is smaller in relativistic fluids than in non-relativistic fluids for the same density dilution ratio across the rarefaction shock. These differences are due to the fact that pressure assumes a larger proportion of the total energy in relativistic fluids when the flow speed gets closer to the speed of light, such as the downstream of rarefaction shocks along reference line b.

Typical shock solutions for relativistic and highly-relativistic fluids are shown in Figure 2. One distinct difference from non-relativistic shocks is that the Rayleigh lines for relativistic fluids are not straight lines any more, which can be easily seen from the form of Equation (12). A more essential difference between relativistic and non-relativistic shocks is that compression shocks $(p_2 > p_1, V_2 < V_1)$ can only be achieved with very high upstream flow speeds in relativistic fluids as indicated for example by the state $(u_1 = 1, v_1 = \frac{1}{\sqrt{2}}c)$ in Figure 2. Furthermore, when the upstream flow speed is reduced by half $(u_1 = 1/2, v_1 = \frac{1}{\sqrt{5}}c)$, only rarefaction shock solution $(p_2 < p_1, V_2 > V_1)$ exists. The criterion distinguishing these two types of shocks is the sound speed of the upstream flow, i.e., $u_1 = \frac{1}{\sqrt{2}}$ and $v_1 = \frac{1}{\sqrt{3}}c$, when the only tangency state between the Rayleigh and Hugoniot lines is the (1,1) point. This classification of shocks and the criterion are the same as those for the non-relativistic shocks.

2.3. Negative pressure downstream flows

Under certain conditions of particle flux (9), the downstream pressure can assume negative values. Take the highly-relativistic case as an example. Combining equations (14) and (17), and by setting the adiabatic index to $\Gamma = 4/3$, we readily obtain the relation

between the reduced downstream pressure and the upstream four-velocity:

$$u_1^2 = \frac{1}{8}(3\hat{p} + 1). \tag{18}$$

Then for upstream velocity in the range $0 < u_1 < \frac{\sqrt{2}}{4}$, the reduced downstream pressure is negative, i.e., $-\frac{1}{3} < \hat{p} < 0$. Furthermore, under this condition the reduced specific volume is an imaginary number according to the highly-relativistic Hugoniot relation (17), i.e., $\hat{V}^2 < 0$. That is, for shock waves in highly-relativistic fluids with a normal upstream flow $(p_1 > 0, V_1 > 0)$ whose speed u_1 is smaller than $\frac{\sqrt{2}}{4}$, a negative pressure state can be achieved in the downstream flow with the specific volume (or density) being an imaginary number. The $\hat{p} - \hat{V}^2$ diagram showing the highly-relativistic shocks with negative-pressure downstream flows $(u_1 = 0.2 \text{ and } 0.3)$ is shown in Figure 3. The physical interpretation of this type of negative pressure fluids with imaginary density (defined as Type I) is not clear so far, although its existence can be ruled out based on entropy considerations, as will be demonstrated in the sequel.

Another type of negative pressure fluids (Type II) is the case of $\Gamma = 2/3$ in the EoS (5), i.e.,

$$p = -\frac{1}{3}\rho\epsilon,\tag{19}$$

which can be interpreted on the basis of dark energy in the universe. Under this equation of state, the combination of highly-relativistic Rayleigh (14) and Hugoniot (17) relations readily leads the form of the upstream four-velocity:

$$u_1^2 = \frac{1}{8}(-3\hat{p} + 1). \tag{20}$$

For the upstream flow speed $u_1 > \frac{\sqrt{2}}{4}$, the reduced pressure is negative, accounting for a negative pressure downstream fluids with the upstream fluids being normal. This type of negative pressure fluids has a real-number specific volume (or density) according to equation (17). Shock waves involving Type II negative pressure fluids are shown in Figure 4.

Entropy analysis showing the availability of these two types of negative pressure fluids are presented in the following.

2.4. Existence of rarefaction shocks

All shock waves should follow the law of entropy increase. Applying the thermodynamic relation (Landau & Lifshitz 1959)

$$d\left(\frac{\omega}{n}\right) = Td\left(\frac{\sigma}{n}\right) + \left(\frac{1}{n}\right)dp \tag{21}$$

in the weak shock wave 2 , we have the following form through Taylor expansion:

$$\frac{\omega_2}{n_2} - \frac{\omega_1}{n_1} = T_1 \left(\frac{\sigma_2}{n_2} - \frac{\sigma_1}{n_1} \right) + \frac{1}{n_1} (p_2 - p_1) + \frac{1}{2} \left(\frac{\partial (1/n)}{\partial p_1} \right)_s (p_2 - p_1)^2 + \frac{1}{6} \left(\frac{\partial^2 (1/n)}{\partial p_1^2} \right)_s (p_2 - p_1)^3. \tag{22}$$

Here T is the temperature, σ the entropy per unit proper volume and $s = \sigma/n$ the entropy per particle. From equation (10), we have another expression of $\frac{\omega_2}{n_2} - \frac{\omega_1}{n_1}$, i.e.

$$\frac{\omega_2}{n_2} - \frac{\omega_1}{n_1} = \frac{1}{2} \left(\frac{1}{n_2} + \frac{1}{n_1} \right) (p_2 - p_1). \tag{23}$$

It should be noticed that in achieving equation (23), the higher order term $\left(\frac{\omega_2}{n_2} - \frac{\omega_1}{n_1}\right)(p_2 - p_1)$ has been omitted. Combining equations (22) and (23), we readily obtain the relation of the entropy difference across the shock front:

$$T_1\left(\frac{\sigma_2}{n_2} - \frac{\sigma_1}{n_1}\right) = \frac{1}{2}\left(\frac{1}{n_2} - \frac{1}{n_1}\right)(p_2 - p_1) - \frac{1}{2}\left(\frac{\partial(1/n)}{\partial p_1}\right)_s(p_2 - p_1)^2 - \frac{1}{6}\left(\frac{\partial^2(1/n)}{\partial p_1^2}\right)_s(p_2 - p_1)^3. \tag{24}$$

By introducing the expansion of $\frac{1}{n_2}$ with respect to $p_2 - p_1$

$$\frac{1}{n_2} - \frac{1}{n_1} = \left(\frac{\partial(1/n)}{\partial p_1}\right)_s (p_2 - p_1) + \frac{1}{2} \left(\frac{\partial^2(1/n)}{\partial p_1^2}\right)_s (p_2 - p_1)^2 \tag{25}$$

²The weak shock wave assumes the discontinuity in every quantity to be small.

to equation (24), we have the simplified expression of the entropy difference across a relativistic shock:

$$\frac{\sigma_2}{n_2} - \frac{\sigma_1}{n_1} = s_2 - s_1 = \frac{1}{12T_1} \left(\frac{\partial^2(1/n)}{\partial p_1^2}\right)_s (p_2 - p_1)^3.$$
 (26)

The law of entropy increase requires that $s_2 - s_1 > 0$.

From the equation of state (5), the particle number density can be expressed as

$$\frac{1}{n} = \frac{(\Gamma - 1)m_0\epsilon}{p}. (27)$$

By using this expression in the entropy equation (26), we have

$$\frac{\sigma_2}{n_2} - \frac{\sigma_1}{n_1} = \frac{(\Gamma - 1)m_0\epsilon_1}{6T_1p_1^3}(p_2 - p_1),\tag{28}$$

from which it is easily identified that for normal upstream fluids with $p_1 > 0$ and $\epsilon_1 > 0$, rarefaction waves with $p_2 - p_1 < 0$ only exist for the adiabatic index $\Gamma < 1$. So under the regime of weak shock, the Type I negative pressure fluids with $\Gamma = 4/3$ does not exist due to the violation of entropy increase law; while Type II negative pressure fluids with $\Gamma = 2/3$ is expected to be a real physical existence. However, since it is still questionable as whether the entropy analysis in weak shocks can be generalized to normal strong shocks, the existence or non-existence of Type I negative pressure fluids in strong shocks needs to be further studied.

3. Relativistic detonation and deflagration waves

When exothermic or endothermic reactions are involved in fluids, detonation or deflagration waves can be excited, which renders the dynamics different from those of non-reactive flows, as will be analyzed in the following.

3.1. Rankine-Hugoniot relations for relativistic combustion waves

Representing the overall energy release per unit mass by q, which is positive and negative for exothermic and endothermic reactions respectively, the specific enthalpies per unit volume across the reaction front³ are

$$\omega_1 = e_1 + p_1 + \rho q \quad \text{and}$$

$$\omega_2 = e_2 + p_2 \tag{29}$$

for upstream and downstream flows, respectively. Following the procedure in deriving Equations (12) and (15), the Rayleigh and Hugoniot relations for relativistic reactive flows are given by:

$$(\hat{p}-1) = -u_1^2 \left[\hat{c}^2 (\hat{V}-1) + \frac{\Gamma}{\Gamma-1} (\hat{p}\hat{V}^2 - 1) - \hat{q} \right], \tag{30}$$

$$\hat{c}^2 \left[\frac{\Gamma+1}{\Gamma-1} (\hat{p}\hat{V}-1) - (\hat{p}-\hat{V}) - 2\hat{q} \right] = \frac{\Gamma}{\Gamma-1} \hat{p} (1-\hat{V}^2) - \frac{\Gamma}{(\Gamma-1)^2} (\hat{p}^2 \hat{V}^2 - 1) + \left(\hat{p} + \frac{\Gamma+1}{\Gamma-1} \right) \hat{q} + \hat{q}^2, \tag{31}$$

where the reduced heat release is $\hat{q} = \frac{\rho_1}{p_1} q$.

Representative Hugoniot lines described by relation (31) are shown in Figure 5. We see that while the non-reactive Hugoniot line passes through the (1,1) point in the $\hat{p} - \hat{V}$ diagram, the Hugoniot lines for flows with exothermic and endothermic reactions are above and below the non-reactive one, respectively. This difference leads to the possible existence of weak detonations in endothermic reactive flows, which will be discussed further when considering Figure 7.

We next note that Rayleigh lines in relativistic reactive fluids do not pass through the (1,1) point in the $\hat{p} - \hat{V}$ diagram (see e.g. Figure 6) as they do in non-reactive relativistic

³The reaction front is normally slim in dimension relative to the entire flow under consideration.

flows (Figure 2). This is because in relativistic reactive flows, the reaction heat release not only is part of the total energy, but it is also present in the momentum conservation equation (see Equations (2) and (29)), which then leads to the presence of the \hat{q} term in the Rayleigh relation (30).

We now separately discuss the solutions for the relativistic detonation and deflagration waves.

3.2. Detonation waves

Detonation wave solutions for relativistic fluids with exothermic and endothermic reactions are shown in Figure 6 and Figure 7, respectively.

Figure 6 shows that detonation solution exists for exothermic reactive fluids with relatively large upstream speeds, i.e., $u_1 \geq \sqrt{2}$; while there is no detonation solution for fluids with relatively slow upstream speed, i.e., $u_1 \leq 1/\sqrt{2}$. However, the criterion of the upstream flow speed for the existence of detonation is higher than the speed of sound⁴, which is different from the case of non-relativistic fluids, for which this criteria is exactly the speed of sound. This is due to the existence of the heat release \hat{q} in the Rayleigh relation (30) for relativistic reactive flows. By numerically exploring Rayleigh lines with different upstream speed u_1 , we find that the criteria for the existence of detonation wave solutions are $u_1 = 1.0$ and $u_1 = 0.9$ for relativistic ($\hat{c} = 1$, $\Gamma = 3/2$) and highly-relativistic ($\hat{c} = 0$, $\Gamma = 4/3$) gases, respectively, both with the energy release $\hat{q} = 1$ (see Figure 6). Another interesting feature is that, while flows with $u_1 = \sqrt{2}$ have both strong and weak detonation solutions, higher speed flows with $u_1 = 4$ have only weak detonation solutions. The reason

⁴In the highly-relativistic fluids, the speed of sound is $u_s = 1/\sqrt{2}$; while in normal relativistic fluids, this value is lower.

for the disappearance of strong detonation for exothermic fluids with high speed upstream flows is that the reaction heat \hat{q} is greatly amplified by the large value of the upstream flow speed u_1 (this is a relativistic effect), which then leads to large pressure compression ratio \hat{p} to satisfy the energy conservation requirement involved in the Hugoniot relation (31).

Detonation solutions in endothermic reactive fluids (Figure 7) are quite different. Only weak detonation can be found, and its solution exists for various upstream flow speeds ranging from subsonic to supersonic. The reason for the extensive existence of weak detonations is that endothermic fluids tend to absorb the fluid kinetic energy of any strength in order to initiate the endothermic reactions (e.g., ionization of the ISM), which then behave as detonations with relatively lower pressure and density compression ratios. In Figure 7, the Rayleigh lines for all upstream flows with different speeds have single intersections with the Hugoniot line, which shows that there is no threshold for the existence of weak detonations. On the other hand, strong detonations cannot be formed for flows with any upstream speed.

3.3. Deflagration waves

Deflagration wave solutions for relativistic fluids with exothermic and endothermic reactions are shown in Figure 8 and Figure 9, respectively.

Figure 8 shows that exothermic reactive fluids have different kinds of deflagration waves for different upstream flow speeds. Specifically, when the upstream flow speed is higher than $u_1 = 0.5$, there is no deflagration solution in both relativistic and highly-relativistic flows. Taking into consideration that no detonation solution exists for exothermic flows with upstream speeds $u_1 \leq 1/\sqrt{2}$ (see Section 3.2 and Figure 6), we conclude that for a certain range of the upstream flow speed (e.g., $1/2 \leq u_1 \leq 1/\sqrt{2}$ in Figure 6 and 8)

in relativistic exothermic reactive fluids, neither detonation nor deflagration waves can form. More specifically, numerical criteria for the existence of deflagration waves have been identified as $u_1 = 0.37$ and $u_1 = 0.39$ for the relativistic and highly-relativistic gases in Figure 8, with the energy release $\hat{q} = 1$. Figure 8 further shows that, for the relatively low upstream speed of $u_1 = 0.3$, both strong and weak deflagrations exit; but when the upstream speed becomes much lower, i.e., $u_1 = 0.2$, strong deflagration cannot be achieved, leaving only the weak deflagration. This can be understood by referring to the Rayleigh relation (30), which shows that as the upstream speed u_1 decreases, the pressure rarefaction ratio \hat{p} (< 1) should be higher for the same reduced specific volume \hat{V} . Then at a certain low value of u_1 , there is no intersection between the Rayleigh and Hugoniot lines for higher \hat{V} , i.e., strong deflagration does not exist.

The wave response is however quite different for endothermic reactive fluids, as shown in Figure 9. No deflagration solution can be found for flows with upstream speeds of $u_1 = 0.2$ and 0.5. Deflagration waves emerge only when the upstream speed is as high as $u_1 = 1.0$ (higher than the sound speed). The numerical criteria for the existence of deflagration waves are $u_1 = 0.7$ and $u_1 = 0.6$ for relativistic and highly-relativistic gases in Figure 9, respectively, with the energy release $\hat{q} = -1$. Referring to the deflagration waves with low upstream speed in exothermic reactive fluids, we expect that endothermic deflagrations need higher upstream flow speeds to propagate. Furthermore, even when the upstream flow speed is higher than the speed of sound, shock cannot form because part of the fluid kinetic energy is absorbed by the endothermic reaction, which is exactly the case of $u_1 = 1.0$ in Figure 9. It is noted (see Section 3.2 and Figure 7) that the existence of weak detonations for a large range of the upstream speed is a distinct feature of endothermic flows. Consequently weak detonation waves, instead of deflagrations, should be the expected dynamic structure in endothermic reactive flows.

3.4. Chapman-Jouguet waves

As a parallel analysis to the non-relativistic Chapman-Jouguet waves, the tangency point of the Rayleigh and Hugoniot lines, representing a limit case of the wave solutions, is analyzed for relativistic fluids. At the tangency point the slopes of Rayleigh and Hugoniot lines are equal to each other, so slopes of both curves in the $\hat{p} - \hat{v}$ diagram are calculated here according to Equations (30) and (31):

$$\left(\frac{d\hat{p}}{d\hat{V}}\right)_{\text{Rayleigh}} = \frac{\hat{c}^2(\hat{p}-1) + 2\frac{\Gamma}{\Gamma-1}\hat{p}\hat{V}(\hat{p}-1)}{\hat{c}^2(\hat{V}-1) + \frac{\Gamma}{\Gamma-1}(\hat{V}^2-1) - \hat{q}},$$
(32)

$$\left(\frac{d\hat{p}}{d\hat{V}}\right)_{\text{Hugoniot}} = -\frac{\hat{c}^2(\frac{\Gamma+1}{\Gamma-1}\hat{p}+1) + 2\frac{\Gamma}{\Gamma-1}\hat{p}\hat{V} + 2\frac{\Gamma}{(\Gamma-1)^2}\hat{p}^2\hat{V}}{\hat{c}^2(\frac{\Gamma+1}{\Gamma-1}\hat{V} - 1) - \frac{\Gamma}{\Gamma-1}(1-\hat{V}^2) + 2\frac{\Gamma}{(\Gamma-1)^2}\hat{p}\hat{V}^2 - \hat{q}}.$$
(33)

And the solution to the relation

$$\left(\frac{d\hat{p}}{d\hat{V}}\right)_{\text{Rayleigh}} = \left(\frac{d\hat{p}}{d\hat{V}}\right)_{\text{Hugoniot}}
\tag{34}$$

shows the criterion of the waves represented by the tangency point. Typical numerical solutions for the Chapman-Jouguet waves as criteria for the existence of detonation waves are given in Section 3.2 and Figure 6 captions.

It is noted that in the non-relativistic extreme of $\hat{c} \to \infty$, the tangency solution degenerates to the normal Chapman-Jouguet wave, i.e.,

$$\frac{\hat{p}-1}{\hat{V}-1} = -\frac{\frac{\Gamma+1}{\Gamma-1}\hat{p}+1}{\frac{\Gamma+1}{\Gamma-1}\hat{V}-1}.$$
(35)

This condition implies that the downstream flow is sonic (c.f. Law 2006), which leads to the classical Chapman-Jouguet wave in which the downstream flow does not affect the the wave front so that the wave propagates steadily. However, no simple solution of the tangency point can be found for relativistic fluids as the heat release \hat{q} are involved in both relations (32) and (33).

3.5. Isobaric waves

A comparison between Figures 6 - 9 and Figure 2 shows that Rayleigh lines for exothermic and endothermic fluids intersect at different points from those of non-reactive fluids in the $\hat{p} - \hat{V}$ diagram. Specifically, in exothermic reactive fluids, the Rayleigh lines intersect at a point with $\hat{p} = 1$ and $\hat{V} > 1$; while for endothermic reactive fluids, the intersection is at $\hat{p} = 1$ and $\hat{V} < 1$. This difference between reactive and non-reactive fluids is caused by the decrease and increase of flow densities in constant-pressure exothermic and endothermic waves, respectively. The example of Figure 7 shows that because the intersection of Rayleigh lines for endothermic reactive fluids is to the right of the Hugoniot line, one can easily achieve weak detonation solutions.

Since the intersections of Rayleigh lines for reactive fluids with different reaction heats \hat{q} have the same reduced pressure $\hat{p} = 1$, we expect the existence of a common solution with $\hat{p} = 1$ for any given reaction heat \hat{q} . Then the Rayleigh relation (30) can be readily converted to the following form by considering $(\hat{p} - 1)$, instead of \hat{p} , as a common factor:

$$(\hat{p} - 1) = \frac{-u_1^2 \left[\frac{\Gamma}{\Gamma - 1} \hat{V}^2 + \hat{c}^2 \hat{V} - (\hat{c}^2 + \hat{q} + \frac{\Gamma}{\Gamma - 1}) \right]}{1 + u_1^2 \hat{V}^2 \frac{\Gamma}{\Gamma - 1}}.$$
 (36)

If we calculate the (positive) \hat{V} root of the numerator in the RHS of this equation, the coordinate of the intersection of the Rayleigh line is

$$\hat{p} = 1, \quad \hat{V} = \frac{\Gamma - 1}{2\Gamma} \left[-\hat{c}^2 + \sqrt{\hat{c}^4 + 4\frac{\Gamma}{\Gamma - 1} \left(\hat{c}^2 + \hat{q} + \frac{\Gamma}{\Gamma - 1} \right)} \right].$$
 (37)

In the non-relativistic limit, $\hat{c} \to \infty$, the intersection is at $(\hat{p} = 1, \hat{V} = 1)$; while in the highly-relativistic limit, $\hat{c} \to 0$, the intersection is at $(\hat{p} = 1, \hat{V} = \sqrt{1 + \frac{\Gamma - 1}{\Gamma}\hat{q}})$. (See Figures 6 - 9 for the variation of the intersection.) In the limiting case of small reaction heat in highly-relativistic fluids, i.e., $\hat{q} = \frac{\rho_1}{p_1} q \ll 1$, the \hat{V} axis of the intersection can be expressed

as $\hat{V} = 1 + \frac{\Gamma - 1}{2\Gamma}\hat{q}$, which can be readily converted to the form of

$$V_2 - V_1 = \frac{\Gamma - 1}{2\Gamma} \frac{q}{p_1}.$$
 (38)

The above equation implies that in an isobaric wave, the specific volume increases and decreases for exothermic and endothermic reactions respectively. In other words, the flow density decreases in an exothermic reaction as the fluid releases energy and increases in an endothermic reaction due to the absorption of energy, if the pressure is kept constant.

3.6. Further considerations of weak detonations and strong deflagrations

Based on entropy considerations, rarefaction shocks normally do not exist for fluids with the adiabatic index $\Gamma > 1$ (cf. Section 2.4, Landau & Lifshitz 1959; Zel'dovich & Raizer 1966), so those weak detonation as well as strong deflagration waves involving rarefaction shocks also normally do not exist. However, in non-relativistic fluids, weak detonation and strong deflagration waves can be found in systems with endothermic reactions or phase transitions, in which a rarefaction shock is not necessary (Axford 1961; Williams 1985). While these understandings still apply in exothermic relativistic detonations and deflagrations, i.e., the weak detonation solutions in Figure 6 and strong deflagration solutions in Figure 8 should normally not exist in realistic systems, there is an exception in that for very high upstream flow speeds (e.g., Rayleigh lines with $u_1 = 4$ in Figure 6), weak detonation waves could exist as no rarefaction shock structure is required in such detonations. Instead, these exothermic weak detonations with high upstream speeds are similar to the weak detonation in endothermic reactive fluids (Figure 7), as both reactions can be directly ignited in the shockless waves because the kinetic energies of the upstream flow is large enough to initiate the reaction. It is therefore reasonable to expect that weak detonation as well as strong deflagration waves of this kind are more common in high-speed astrophysical flows, and they are expected to have different structures from the

traditional Zel'dovich - von Neumann - Döring (ZND) structure in strong detonation waves (cf. Williams 1985). One such example is that of relativistic endothermic reactive fluids, for which weak detonation waves instead of weak deflagration waves are the dominant dynamics as can be seen from Figure 7 and Figure 9.

We further note that the non-relativistic form of endothermic combustion waves has been studied for interstellar gas ionization (Axford 1961). The ionization of neutral hydrogen atoms is an endothermic reaction which forms an 'ionization front' in the interstellar media. This front, separating the unionized (H I) and the fully ionized (H II) regions, is dynamically identical to the detonation (or deflagration) front. Axford (1961) has shown the existence of both weak detonation and strong deflagration waves theoretically and what we discussed here is a generalization of these results to the relativistic regime. Besides the ionization of neutral hydrogen atoms around hot stars, the re-ionization (also of neutral hydrogen atoms by stars and quasars) process of the universe (Miralda-Escudé 2003) can also be considered as an endothermic combustion wave. Another endothermic fluid process in astrophysics is the inverse Compton scattering, the mechanism for a large variety of high energy X-ray and γ -ray radiations (e.g., De Jager & Harding 1992; Tavani 2011).

For relativistic fluids with Γ < 1, rarefaction shocks are allowed through entropy consideration (cf. Section 2.4), and as such lead to the formation of weak detonations. This is obviously another way of having weak detonations in astrophysical relativistic fluids.

4. Conclusions

As a theoretical foundation to study the dynamics of astrophysical systems, the basis of relativistic reactive fluid dynamics is formulated here in terms of the Rankine-Hugoniot relations for detonation and deflagration waves in normal relativistic reactive flows. The relativistic shock theory is revisited and the mathematical solutions of two types of negative pressure downstream flows are identified. Normal relativistic and highly-relativistic detonation and deflagration wave solutions are constructed for both exothermic and endothermic reactive flows. The existence of endothermic reactions in astrophysical phenomena extends the family of potentially realizable combustion waves in terms of weak detonations and strong deflagrations, which do not exist extensively in terrestrial situations. These theoretical results can be applied in astrophysical systems such as supernovae explosions, γ -ray bursts and the false vacuum decay in the early universe, for which the conventional shock theories do not hold.

This work was supported by the start up fund for the Center for Combustion Energy at Tsinghua University and the National Science Foundation of China (NSFC 51206088). YG in addition acknowledges support from the China Postdoctoral Science Foundation No. 2011M500313.

REFERENCES

Akkerman, V., Law, C. K., & Bychkov, V. 2011, Phys. Rev. E, 83, 026305

Anile, A. M. 1989, Relativistic fluids and magneto-fluids: with applications in astrophysics and plasma physics (New York; Cambridge University Press)

Arnett, W. D. 1969, Ap&SS, 5, 180

Axford, W. I. 1961, Phil. Trans. R. Soc. London, A, 253, 301

Blandford, R. D., & Ostriker, J. P. 1978, ApJ, 221, L29

Blandford, R. D., & Ostriker, J. P. 1980, ApJ, 237, 793

Burrows, A. 2000, Nature, 403, 727

Cissoko, M. 1997, Phys. Rev. D, 55, 4555

De Jager, O. C., & Harding, A. K. 1992, ApJ, 396, 161

Evans, N. J., II 1999, ARA&A, 37, 331

Flower, D. R., & des Forêts, G. P. 2010, MNRAS, 406, 1745

Gamezo, V. N., Khokhlov, A. M., Oran, E. S., Chtchelkanova, A. Y., & Rosenberg, R. O. 2003, Science, 299, 77

Gamezo, V. N., Khokhlov, A. M., & Oran, E. S. 2005, ApJ, 623, 337

Gao, Y., & Law, C. K. 2011, Phys. Rev. Lett., 107, 171102,

Gibson, C. H. 2005, Combust. Sci. and Tech., 177, 1049

Gusdorf, A., des Forêts, G. P., Cabrit, S., & Flower, D. R. 2008, A&A, 490, 695

Gyulassy, M., Kajantie, K., Kurki-Suonio, H., & McLerran, L. 1984, Nucl. Phys. B, 237, 477

Hillebrandt, W., & Niemeyer, J. C. 2000, ARA&A, 38, 191

Ivanova, L. N., Imshennik, V. S., & Chechotkin, V. M. 1974, Ap&SS, 31, 497

Jørgensen, J. K., Hogerheijde, M. R., Blake, G. A., van Dishoeck, E. F., Mundy, L. G., & Schöier, F. L. 2004, A&A, 415, 1021

Kennel, C. F., & Coroniti, F. V. 1984, ApJ, 283, 694

Khokhlov, A. M. 1989, MNRAS, 239, 785

Khokhlov, A. M. 1991, A&A, 245, 114

Klein, R. I., McKee, C. F., & Colella, P. 1994, ApJ, 420, 213

Landau, L. D., & Lifhshitz E. M. 1959, Fluid Mechanics (New York; Pergamon Press)

Lanza, A., Motta, S., & Miller, J. C. 1982, Nuovo Cimento, Lettere, 35, 309

Law, C. K. 2006, Combustion Physics (New York; Cambridge University Press)

Liang, E. P. T. 1977, ApJ, 211, 361

Mallick, R. 2011, Phys. Rev. C., 84, 065805

McKee, C. F., & Ostriker, E. C. 2007, ARA&A, 45, 565

Mészáros, P. 2001, Science, 291, 79

Mészáros, P. 2002, ARA&A, 40, 137

Miralda-Escudé, J. 2003, Science, 300, 1904

Mitchell, G. F., & Deveau, T. J. 1983, ApJ, 266, 646

Newman R. C., & Axford, W. I. 1968, ApJ, 151, 1145

Nomoto, K., Sugimoto, D., & Neo, S. 1976, Ap&SS, 39, L37

Poludnenko, A. Y., Gardiner, T. A., & Oran, E. S. 2011, Phys. Rev. Lett., 107, 054501

Steinhardt, P. J. 1982, Phys. Rev. D, 25, 2074

Synge, J. L. 1957, The Relativatic Gas (Amsterdam; North-Holland Publishing Company)

Taub, A. H. 1948, Phys. Rev., 74, 328

Tavani, M., Bulgarelli, A., Vittorini, V., et al. 2011, Science, 311, 736

Williams, F. A., 1985, Combustion Theory (2nd ed.; Menlo Park, Ca; The Benjamin/Cummings Publishing Company, Inc.)

Woosley, S. E., & Weaver, T. A. 1986, ARA&A, 24, 205

Woosley, S. E., Kerstein, A. R., & Aspden, A. J. 2011, ApJ, 734, 37

Yorke, H. W. 1986, ARA&A, 24, 49

Zel'dovich, Ya. B., Raizer Yu. P. 1966, Physics of Shock Waves and High-Temperature Hydrodynamic Phenomena, (New York, Academic Press)

Zel'dovich, Ya. B., Barenblatt, G. I., Librovich, V. B. & Makhviladze, G. M. 1985, The Mathematical Theory of Combustion and Explosions, (Eng. ed.; New York; Mcneill D. H., Consultants Bureau)

This manuscript was prepared with the AAS LATEX macros v5.2.

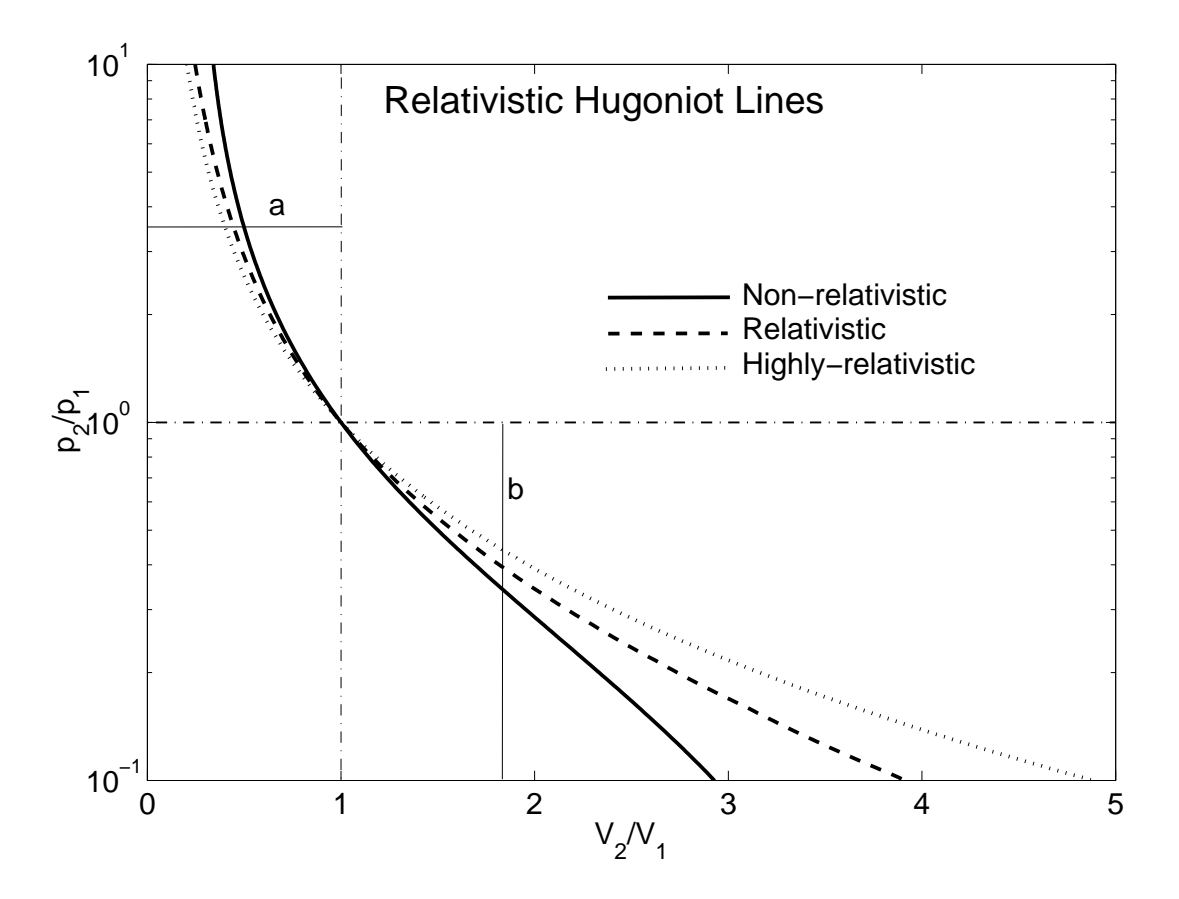


Fig. 1.— Hugoniot lines for non-relativistic (Equation (16) with $\Gamma = 5/3$), relativistic (Equation (15) with $\hat{c} = 1$ and $\Gamma = 3/2$) and highly-relativistic fluids (Equation (17) with $\Gamma = 4/3$). The ordinate is the downstream pressure relative to the upstream one; the abscissa is the downstream specific volume relative to the upstream value. All curves pass through the point (1,1). We notice that for the same downstream to upstream pressure compression ratio (reference line a), the density increase is higher for relativistic fluids than for non-relativistic fluids; while for the same downstream to upstream density diluent ratio (reference line b), the pressure reduces less in relativistic fluids than in non-relativistic fluids.

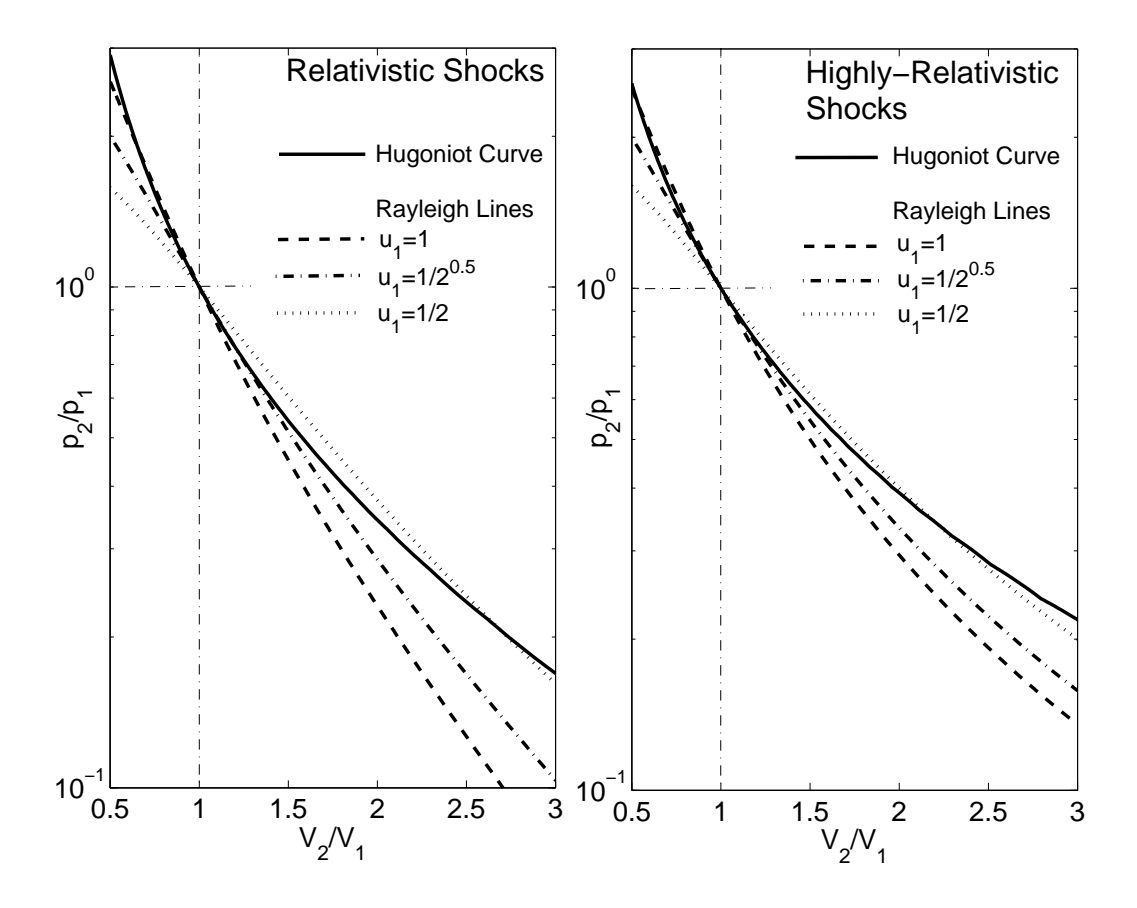


Fig. 2.— Rankine-Hugoniot shock solutions for relativistic ($\hat{c}=1,\ \Gamma=3/2$) and highly-relativistic ($\hat{c}=0,\ \Gamma=4/3$) fluids in the $\hat{p}-\hat{V}$ diagram. The Rayleigh lines are not straight lines as they are in the non-relativistic case (see, e.g., Landau & Lifshitz 1959). We can see that for (highly-)relativistic fluids, compression shocks with $p_2/p_1>1$ can only be achieved for relatively higher upstream fluid speeds (here $u_1=1$ for example). And for relatively lower upstream fluid speeds (here $u_1=1/2$ for example), only "rarefaction shocks" with $p_2/p_1<1$ (which normally do not happen due to entropy increase) exist. In between these two kinds of shocks is the sound-speed-upstream-flow, i.e., the Rayleigh line with $u_1=1/\sqrt{2}$, which does not have any shock solution.

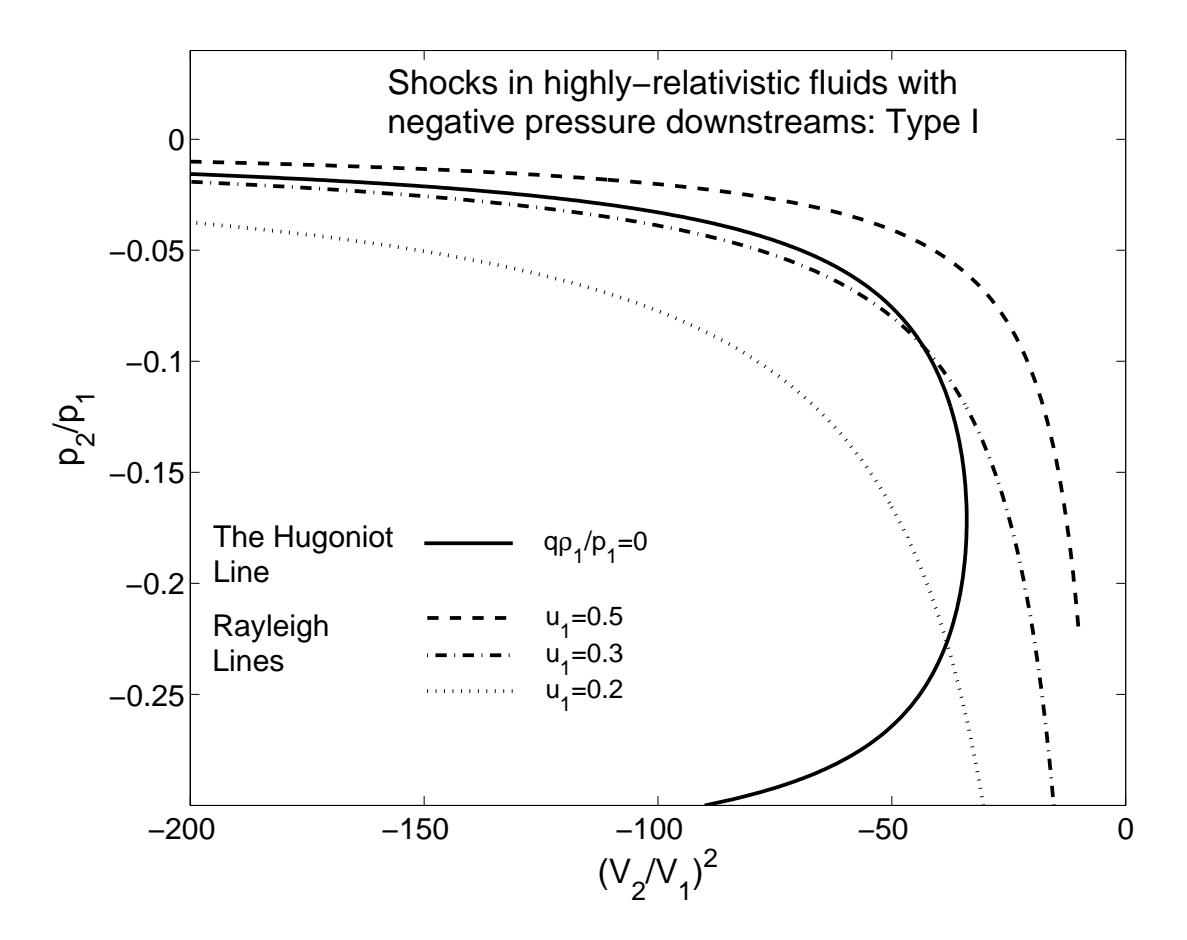


Fig. 3.— Shock solutions for highly-relativistic ($\hat{c}=0$, $\Gamma=4/3$) fluids in the $\hat{p}-\hat{V}^2$ diagram with negative pressure downstream flows. The square of the specific volume is also a negative value, which means that the downstream specific volume (or density) is an imaginary number if we assume the upstream flow to be normal fluids. We can see that there is no intersection between the Hugoniot line and the Rayleigh line with $u_1=0.5$, while intersections exist for Rayleigh lines with $u_1=0.2$ and $u_1=0.3$. In fact, for highly-relativistic fluids, only when the upstream flow speed is in the range of $0 < u_1 < \frac{\sqrt{2}}{4}$ (see Section 2.3) can we achieve negative pressure flows via this kind of shocks. However all this shocks do not follow the entropy increase law (cf. Section 2.4) so this Type I negative pressure fluids physically do not exist.

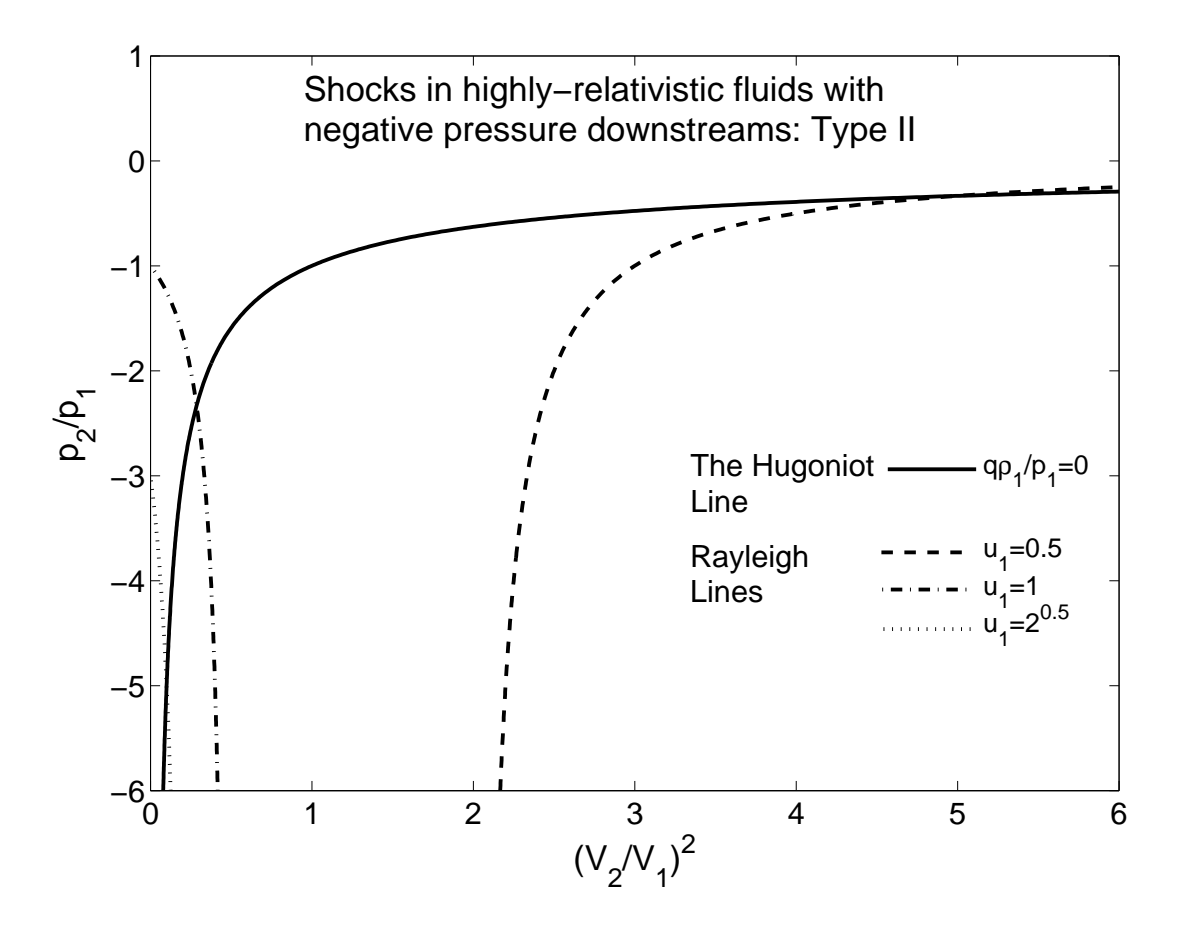


Fig. 4.— Shock solutions for highly-relativistic ($\hat{c}=0$, $\Gamma=2/3$) fluids in the $\hat{p}-\hat{V}^2$ diagram with negative pressure downstream flows. Shock solutions exist for Rayleigh lines with upstream speeds in the range of $u_1 > \frac{\sqrt{2}}{4}$, i.e., $u_1 = 0.5$, $u_1 = 1.0$ and $u_1 = \sqrt{2}$. These Type II negative pressure fluids follow the entropy increase law (cf. Section 2.4) thus are physically available.

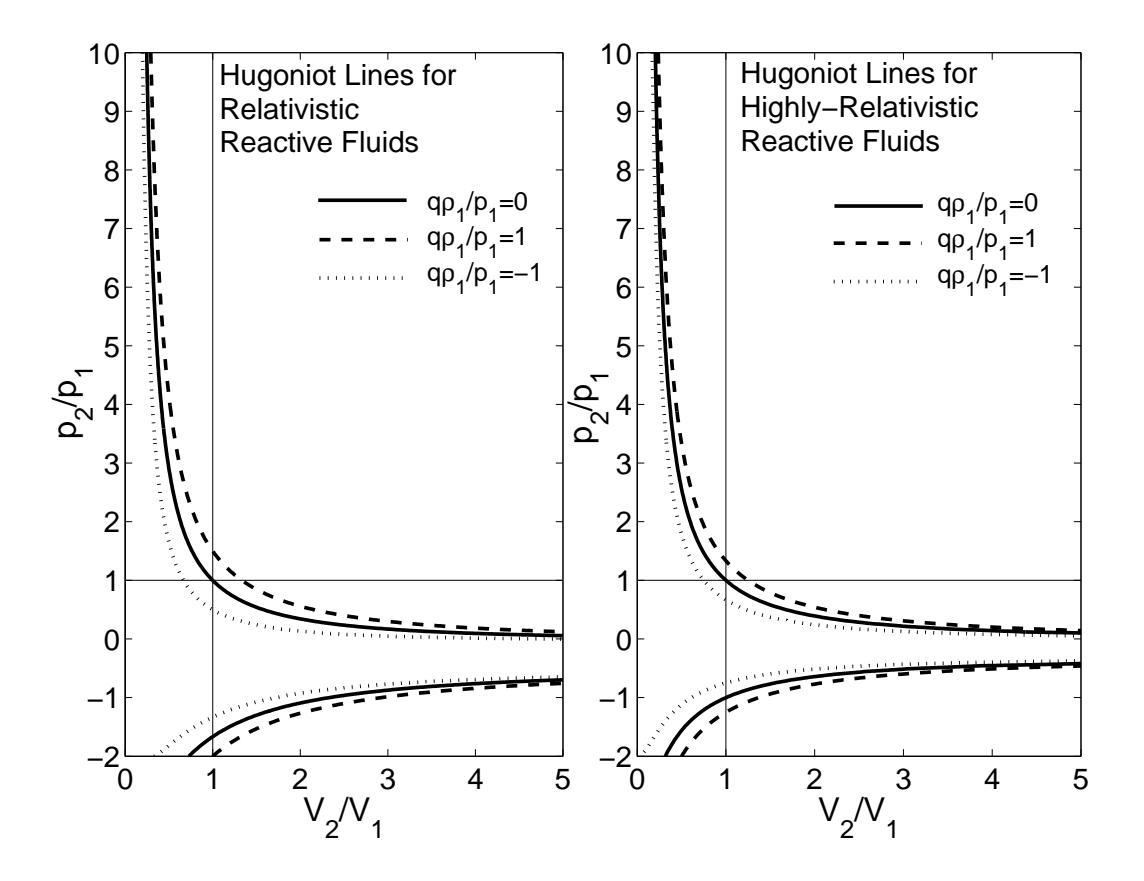


Fig. 5.— Hugoniot lines for relativistic gas ($\hat{c} = 1$, $\Gamma = 3/2$) and highly-relativistic gas ($\hat{c} = 0$, $\Gamma = 4/3$). In the first quadrant, the Hugoniot line with positive reaction energy (here q = 1 for example) is above the shock Hugoniot line with q = 0, and the Hugoniot line with endothermic reaction (here q = -1 for example) is below the shock Hugoniot line. It is also noted that Hugoniot lines are also present in the forth quadrant, hence allowing the existence of shock or reactive wave solutions with negative pressures fluids. One such shock solution has been demonstrated in Figure 4.

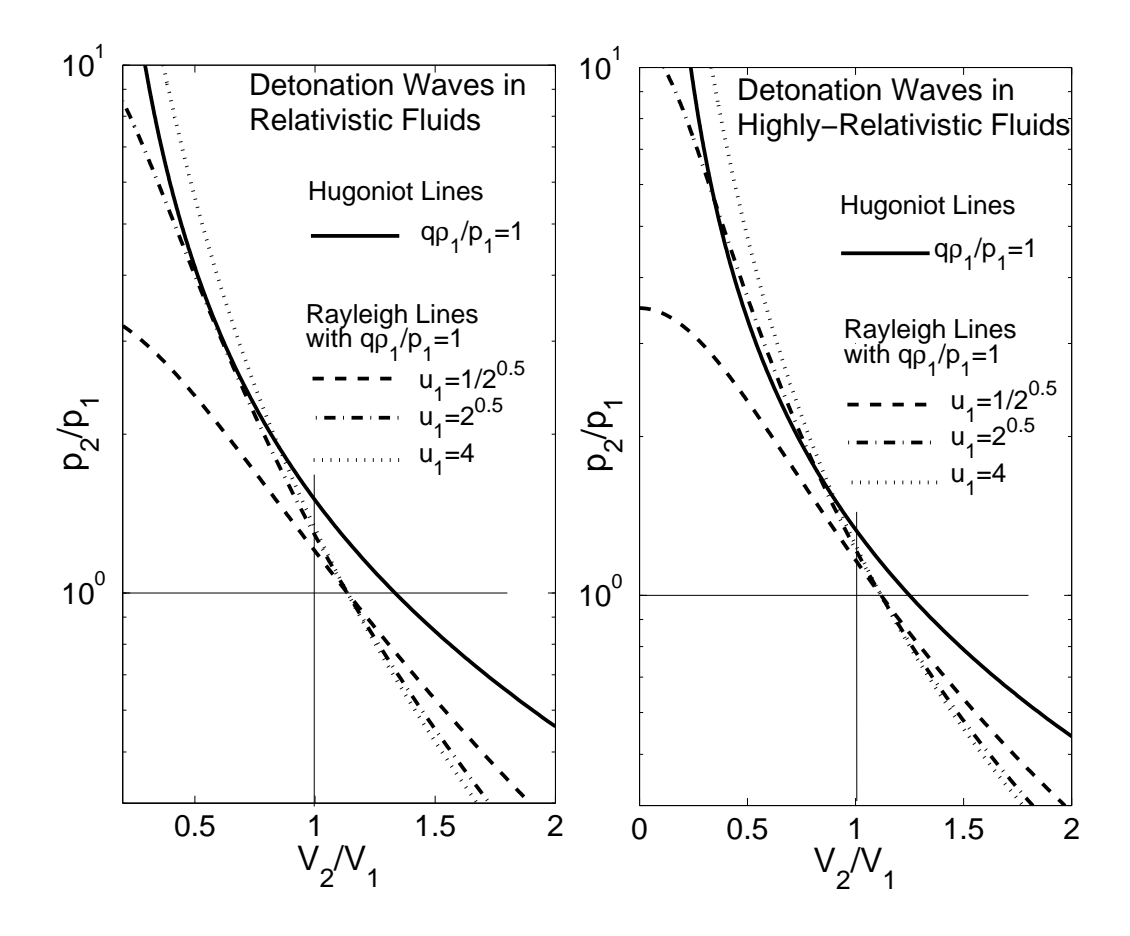


Fig. 6.— Detonation wave solutions for relativistic gas ($\hat{c}=1,\ \Gamma=3/2$) and highly-relativistic gas ($\hat{c}=0,\ \Gamma=4/3$) with an exothermic reaction ($\hat{q}=1$). For relatively low-speed fluids with $u_1=1/\sqrt{2}$, there is no intersection between the Rayleigh lines and the Hugoniot lines with $\hat{q}=1$, i.e., no exothermic detonation wave exist. For intermediate-speed fluids with $u_1=\sqrt{2}$, binary intersections can be found between the Rayleigh lines and the Hugoniot lines, implying the existence of both strong and weak detonations for the exothermic reactive flows. For high-speed fluids with $u_1=4$, there are only single intersections between the Rayleigh lines and Hugoniot lines, which are weak exothermic detonations. The criteria for the existence of detonation waves are $u_1=1.0$ and $u_1=0.9$ for the left and right panels, respectively, as obtained from numerical explorations. It is also noticed that for both the left and right panels, all Rayleigh lines intersect at a point with $\hat{q}=1$ and $\hat{V}>1$.

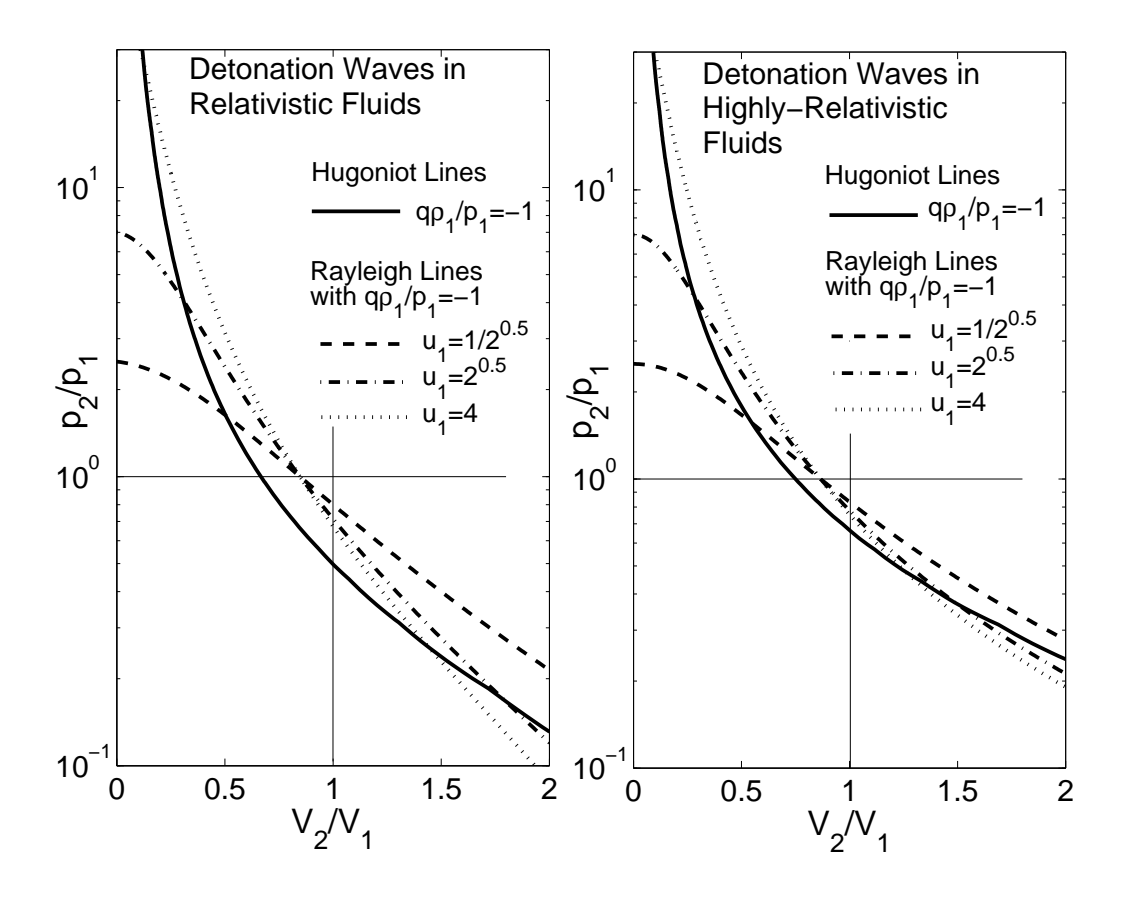


Fig. 7.— Detonation wave solutions for relativistic gas ($\hat{c}=1,\ \Gamma=3/2$) and highly-relativistic gas ($\hat{c}=0,\ \Gamma=4/3$) with an endothermic reaction ($\hat{q}=-1$). The ordinates are in the logarithm coordinates. For fluids with all upstream speeds shown here ($u_1=1/\sqrt{2},\ u_1=\sqrt{2}$ and $u_1=4$), there are single intersections between the Rayleigh lines and Hugoniot lines with $\hat{q}=-1$ in the detonation region ($\hat{p}>1$), which means that weak endothermic detonations always exist. In both panels, Rayleigh lines intersect at a point with $\hat{q}=1$ and $\hat{V}<1$.

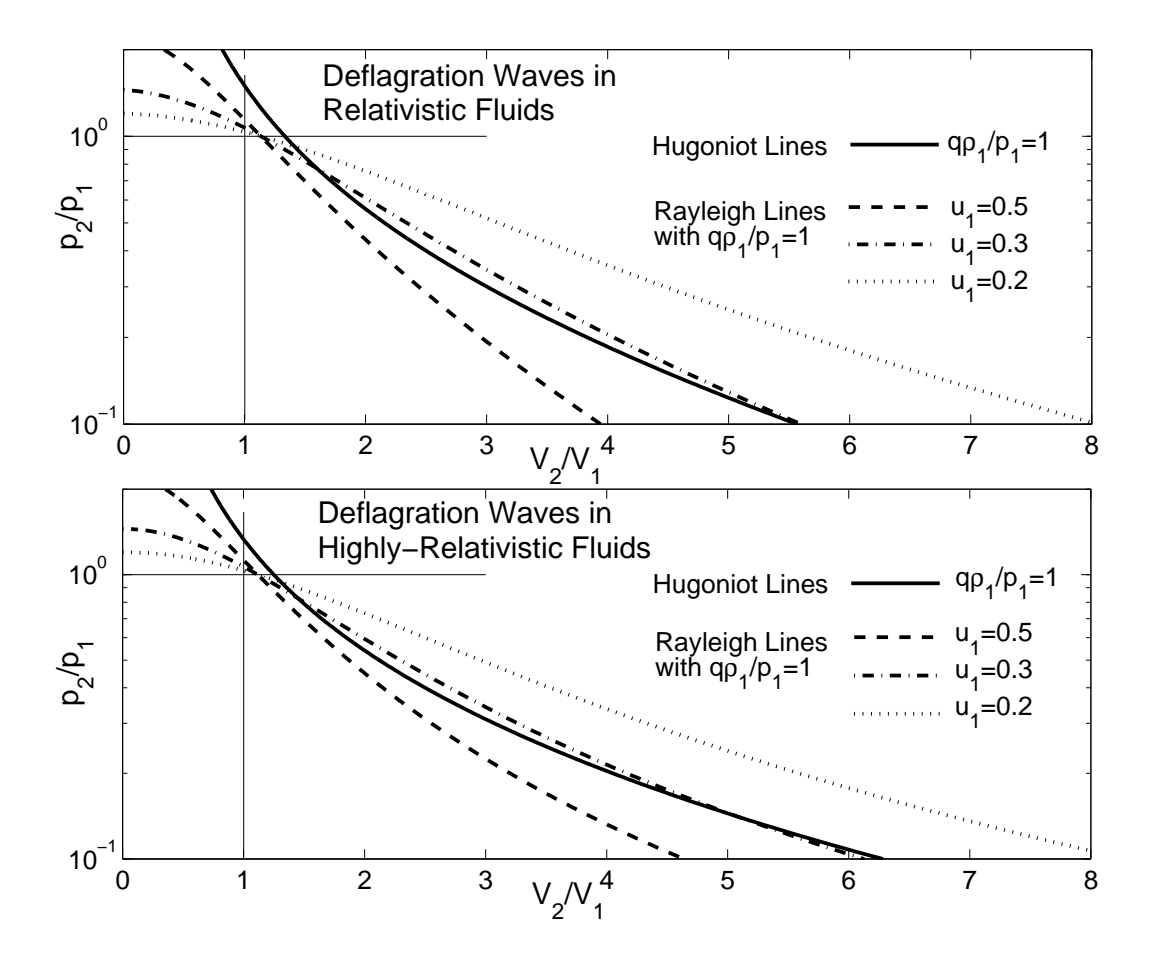


Fig. 8.— Deflagration wave solutions for relativistic gas ($\hat{c}=1,~\Gamma=3/2$) and highly-relativistic gas ($\hat{c}=0$ and $\Gamma=4/3$) with an exothermic reaction ($\hat{q}=1$). For relatively high-speed fluids with $u_1=0.5$, there is no intersections between the Rayleigh lines and the Hugoniot lines with $\hat{q}=1$, i.e., there is no deflagration waves. For intermediate-speed fluids with $u_1=0.3$, binary intersections can be found between the Rayleigh lines and Hugoniot lines with $\hat{q}=1$, implying the existence of both strong and weak deflagrations for the exothermic reactive flows. For low-speed fluids with $u_1=0.2$, there are only single intersections between the Rayleigh lines and Hugoniot lines with $\hat{q}=1$, representing strong exothermic deflagrations. The criteria for the existence of deflagrations in the upper and lower panels are $u_1=0.37$ and $u_1=0.39$, respectively, as obtained from numerical explorations. In both panels, Rayleigh lines intersect at a point with $\hat{q}=1$ and $\hat{V}>1$.

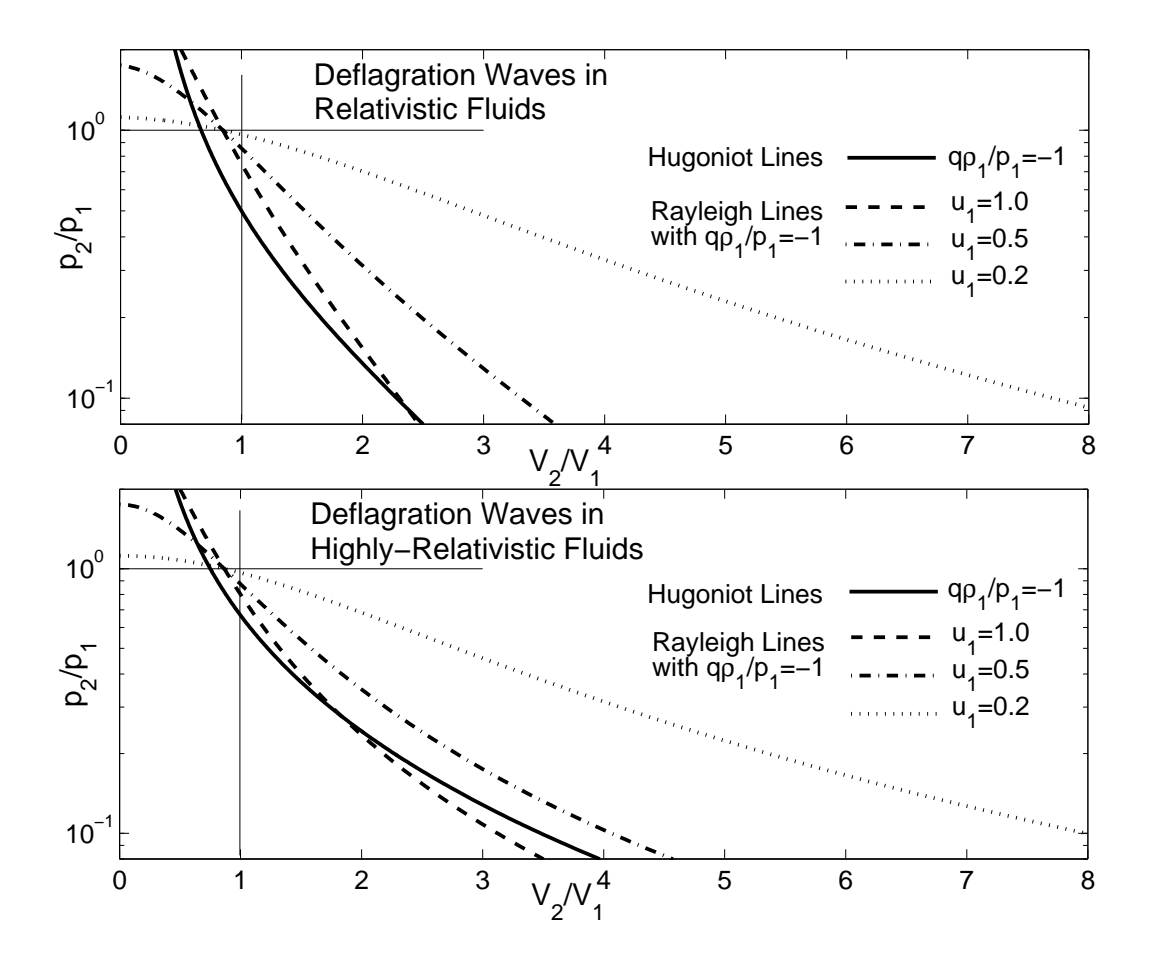


Fig. 9.— Deflagration wave solutions for relativistic gas ($\hat{c}=1,~\Gamma=3/2$) and highly-relativistic gas ($\hat{c}=0,~\Gamma=4/3$) with an endothermic reaction ($\hat{q}=-1$). For low-speed flows with $u_1=0.2$ and $u_1=0.5$, there is no intersection between the Rayleigh lines and Hugoniot lines with $\hat{q}=-1$ in the deflagration region ($\hat{p}<1$), which means that endothermic deflagrations do not exist. For relatively-high-speed flows with $u_1=1.0$, there are intersections between the Rayleigh lines and Hugoniot lines with $\hat{q}=-1$ in the deflagration region ($\hat{p}<1$), representing the existence of endothermic deflagrations. Numerical explorations show that the criteria for the existence of deflagrations are $u_1=0.7$ and $u_1=0.6$ for the upper and lower panels, respectively. In both panels, Rayleigh lines intersect at a point with $\hat{q}=1$ and $\hat{V}<1$.